Available online at www.sciencedirect.com
SCIENCE DIRECT®
Robotics and Autonomous Systems 50 (2005) 13–25
Robotics and Autonomous Systems
www.elsevier.com/locate/robot

Differentiating walls from corners using the amplitude of ultrasonic echoes

Ginés Benet*, Milagros Martínez, Francisco Blanes, Pascual Pérez, José E. Simó

Departamento de Informática de Sistemas y Computadores, Universidad Politécnica de Valencia, P.O. Box 22012, 46080 Valencia, Spain

Received 27 March 2003; received in revised form 16 June 2004; accepted 8 July 2004
Available online 28 August 2004

Abstract

This paper analyzes the use of ultrasonic echo amplitudes to evaluate the characteristics of the detected surfaces (such as distinguishing between walls and corners). The shape and surface characteristics of the environment, such as roughness or absorption coefficient, as well as the distance and the angle of incidence, have high influence on the amplitude of the echoes. As a consequence, the amplitude of the received echoes has received little attention from robotic researchers. Instead, time-of-flight (ToF) has been used as the main source of information of the environment. It is also well known that the shape of the echoes of a corner is the same as that of a wall [IEEE Trans. Pattern Anal. Mach. Intell. (PAMI), 12 (1990) 560]. Several authors have proposed special multi-transducer configurations to avoid this problem. This paper studies the amplitude of received echoes and presents a simple model to predict the shape and amplitude of echoes received from different materials in environments composed of walls and corners. Using this model, and analysing the amplitude of the echoes it is possible to distinguish between walls and corners in a single scan of a single ultrasonic transducer pair. The parameters of the model were obtained from tests performed on different materials and surfaces. The last section of the paper shows the experimental results of the wall–corner classifications obtained in real tests during the walk of a mobile robot. The results suggest that the method proposed can be of great interest for map building in robotics.

Keywords: Ultrasonic sensors; Amplitude response model; Map building; Mobile robots

1. Introduction

Ultrasonic sensors are widely used in robotics to avoid collisions and for map building purposes. They have some advantages over laser or camera: they are low-cost and low-power consuming, they are not light dependent and, moreover, the ultrasonic signal is low bandwidth and hence its data processing requirements

* Corresponding author. Tel.: +34 96 387 7578; fax: +34 96 387 7579.
E-mail addresses: gbenet@disca.upv.es (G. Benet), mimar@disca.upv.es (M. Martínez), pblanes@disca.upv.es (F. Blanes), pperez@disca.upv.es (P. Pérez), jsimo@disca.upv.es (J.E. Simó).

0921-8890/$ – see front matter © 2004 Elsevier B.V. All rights reserved.
doi:10.1016/j.robot.2004.07.011

are reduced. On the other hand, there are some disadvantages: environmental temperature affects wave absorption; wide beam width (from 30 to 60°) of the ultrasonic transducer lobe yields imprecise angular measurements, low bandwidth also means low distance resolution, making close objects indistinguishable.

Several characteristics of the received ultrasonic echoes have been used to obtain the environment features. The most common are based on the time elapsed between transmission and reception of a pulse ("time-of-flight" (ToF)) [1,23]. The duration of the echo and its energy are analysed in [16], and the phase differences are used in [8,10]. A combination of ToF and echo amplitude is used in [15,24], and a combination of frequency, echo amplitude and ToF is used in [2,12]. A significant amount of early work on sonar-based mapping was done by Elfes [6] and Elfes and Moravec [21]. In these papers, probabilistic grid maps were obtained using an ultrasonic ring. Each cell in the map was associated with probability density functions for occupied, empty and unknown situations.

Kleeman and Kuc [13] stated that "two transmitters and two receivers are necessary and sufficient for discriminating planes, corners, and edges in two dimensions". This is true if only echo ToFs are used. In the literature, we can find several transducer configurations that exploit geometric properties of ultrasonic signal reflection to discriminate between planes and corners with a single scan, as described in [3,9,14]. But, if only one transmitter/receiver pair is used, two measurements from different locations will be needed for feature extraction [17,18].

The aim of this paper is to analyse the ultrasonic echo amplitude, as this information can be added to ToF in order to obtain more information from the environment. Echo amplitude could be added to conventional information, such as range and incidence angle, to perform geometric feature differentiation. The sonar system has only an ultrasonic sensor pair (T/R), and only a single circular scan is needed.

The paper is structured as follows: Section 2 describes some considerations about the amplitudes of the ultrasonic echoes; Section 3 presents an echo amplitude response model, used to predict echo amplitudes when the surface reflection coefficient C_r is known; Section 4 describes the measuring system, and its main characteristics; Section 5 shows the application of the echo amplitude response model for wall–corner differentiation; and finally, in Section 6, the results obtained from several validation tests are presented and discussed.

2. Considerations about the amplitude of ultrasonic echoes

The amplitude of the ultrasonic echoes depends on several factors: distance, surface characteristics of the reflector, viewing angle and shape of the reflector surface. The following sections describe these factors, introducing the equations used to model the ultrasonic signal amplitude.

2.1. Distance

Ultrasonic signal propagates through air and the intensity of the signal decreases with distance due to two main reasons: beam spreading and air absorption. Thus, the signal amplitude obtained in a receiver placed at a distance x from the transmitter will decrease as x increases. In the bibliography, this decay in the amplitude of ultrasonic signal has been modelled using different expressions [4,22,24]. In [5], Cracknell indicates that ultrasound attenuation in air has two factors: one exponential, due to air absorption, and the other, hyperbolic, due to beam spreading. This can be expressed as:

$$A(x) = A_0 \frac{e^{-\alpha x}}{x} \tag{1}$$

where A_0 is a constant, α the attenuation coefficient of the air (dB m^{-1}), x the distance between emitter and receiver (m).

It is difficult to accurately measure the attenuation coefficient, α, as it depends on several factors, the most important being air density, air temperature, and the square of the signal frequency (f). The following formula for α in dry air at 0 °C is given in [5]:

$$\alpha_{\text{air}}\,(\text{dB m}^{-1}) = 1.61 \times 10^{-8} \times f^2$$

Thus, for $f = 40$ kHz, the following value is obtained:

$$\alpha_{\text{air}} = 0.257\,\text{dB m}^{-1} \quad (\text{dry air at } 0\,^{\circ}\text{C})$$

Eq. (1) has been selected in the present work to model ultrasound amplitude decrease in air because it agrees well with the experimental data obtained. Exhaustive tests were carried out in the laboratory using 40 kHz Massa piezo-ceramic transducers, for distances

ranging from 0.6 to 3 m, at air temperatures ranging between 23 and 25 °C, relative humidity of 60%. Under these conditions, the value for α was obtained using least squares adjustment, yielding: $\alpha_{\text{air}} = 0.275 \pm 0.0018\,\text{dB m}^{-1}$, with a correlation coefficient of 0.935.

2.2. Surface characteristics of the reflector

In robotic applications, objects are detected when the ultrasonic beam produced in a robot's transmitter reaches a solid surface, and is scattered back to the receiver's transducer, located also in the robot. In the case of Polaroid transducers, the same device can be used both as a receiver and as a transmitter. In our case, a piezo-ceramic transmitter–receiver transducer pair is used.

The way these reflections occur is similar to that of a mirror, but depending on the density and surface finish, the reflected beam will experience additional spreading. In addition, only a fraction of the incident energy is reflected, reducing the intensity of the reflected beam. Thus, a polished surface will produce less beam spreading than a rough surface. Also, other physical properties of the surface, such as relative density, modify the percentage of the incident energy that will be reflected back. That is, only a reduced fraction of the energy emitted from the transmitter will arrive at the receiving transducer after reflection. This fraction of energy will depend mainly on the physical surface properties [19].

Taking into account these factors, a simple reflection coefficient C_{r} is proposed to model the total intensity reduction of the ultrasonic beam reflected on a surface. Thus, a given object with a uniform surface finish will be modelled as a surface with a quasi-constant reflection coefficient C_{r}, as expressed in the following equation:

$$C_{\text{r}} = \frac{A_{\text{reflected}}}{A_{\text{incident}}}, \tag{2}$$

where C_{r} is the surface reflection coefficient, a numerical value ranging between 0 and 1, and $A_{\text{reflected}}$ and A_{incident} are the intensity of the reflected and incident ultrasonic beams, respectively.

Thus, using Eqs. (1) and (2), the amplitude of an ultrasonic echo received after reflection in a normal plane of a surface with reflection coefficient C_{r}, placed at distance x, will be expressed as:

$$A(x) = A_0 C_{\text{r}} \frac{e^{-2\alpha x}}{2x}. \tag{3}$$

(Note that $2x$ is the total path length travelled by the ultrasonic signal).

2.3. Transducers orientation

The ultrasonic transducer pair has different amplitude responses depending on the incidence angle (θ) at which the target is viewed by the transducer, showing a maximum value A_{max} of received echoes when this angle is zero. (In the case of a flat surface, like in a wall, the target point will be the one viewed by the transducer in a direction normal to the wall). The peak amplitude of the received echoes decreases as the angle increases, but the distance (time-of-flight) will be the same for all of them. Thus, if a circular scan is performed in a scene with a single object (i.e. a flat wall, or a vertical rod), for each transducer's orientation an echo will be received with the same time of flight, corresponding to the distance between the transducers and the target. However, the peak amplitude of the echoes will follow a Gaussian-like shape, as can be seen in Fig. 1. In [14], Kuc presents a formula that models this dependence of amplitude evolution with the viewing angle θ:

$$A(\theta) = e^{-4\theta^2/\theta_0^2} \tag{4}$$

where θ_0 is the angle that produces a value for $A \cong 0.02$ times A_{max}. This formula agrees well with the real response of the transducers used. In Fig. 1, the normalised real angular response of the ultrasonic transducers used in the experiments, has been plotted, together with the normalised plot of the values obtained from Eq. (4), with $\theta_0 = 50°$. As can be seen in Fig. 1 the beam width of the angular response lobe (that is, the angle corresponding to a value of $0.5\times A_{\text{max}}$) is of $\pm 21°$ for the transducers used in this work.

Thus, from the angular shape of the echoes received in a circular scan, the normal incidence point (referred to in this article as *target point*) can be easily located for each surface, finding the maximums of the scanned signal. The position of this maximum in the time axis will give us its range, and its position on the angle axis will give us the angular position where the target has its normal orientation. This

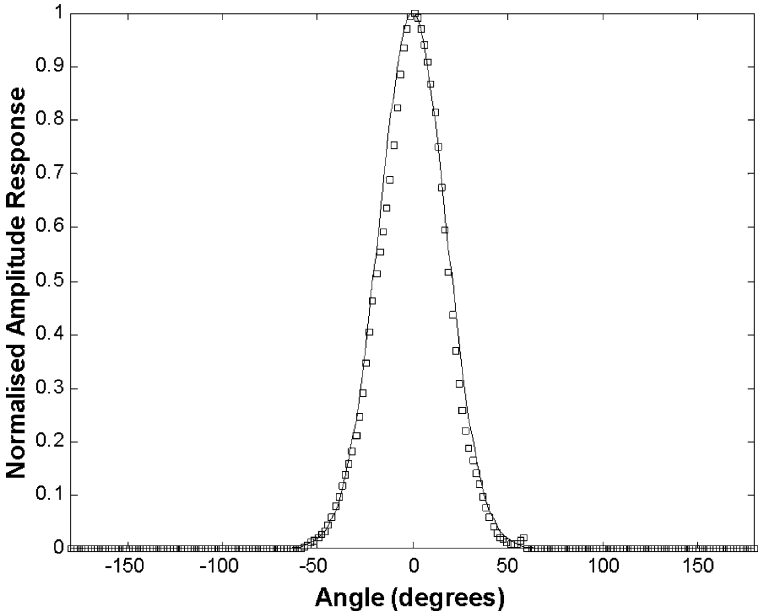

Fig. 1. Normalised shape of the angular response of the amplitude peaks of echoes received in a circular ultrasonic scan with a wall of concrete placed in front of the transducers. Squares: measured values; solid line: the corresponding model of Eq. (4), with $\theta_0 = 50^\circ$.

fact has been used by some authors for map building and for target localisation [11,12] and constitutes an interesting method to establish geometric features of maps.

2.4. Shape of reflecting surfaces

Commonly three types of features are extracted from the environments wherein the robot usually navigates: walls, right corners and edges. In our experiments, edges produce small amplitude echoes of the same order of magnitude as noise, making them undetectable. For this reason, this paper will focus only on walls and corners as the main features to be extracted from the environment.

Some differences between edges, walls and corners scanned shapes were described in [23]. However, other authors have reported that the peak amplitudes of echoes reflected from walls and from right corners, for the same type of material, distance and incidence angle, have almost the same shape [24]. In fact, the numerous samples taken from real environments have shown that there are not meaningful differences between the angular responses of a corner and of a wall located at the same distance.

Nevertheless, it is still possible to find out differences between echo reflections from each reflector type. As can be seen in Fig. 2, the echo reflection from a wall and the echo reflection from a right corner are different in a substantial aspect: wall-reflected echoes only touch the surface once, whereas corner-reflected echoes are reflected twice during their flight towards the receiver. Thus, signal absorption will not be the same, and some additional dispersion will be added to the reflected beam. This suggests an interesting conclusion, presented in this paper: "*a corner will always produce smaller echo amplitudes than a wall of the same characteristics placed at the same distance*".

3. Amplitude response model: parameters of the model

As indicated in Section 2, the ultrasonic echo amplitude depends on several parameters. This amplitude behaviour can be easily modelled using a simplified equation:

$$A = A_0 C_{\mathrm{r}}^N \frac{e^{-2\alpha x}}{2x} e^{(-4\theta^2/\theta o^2)}, \tag{5}$$

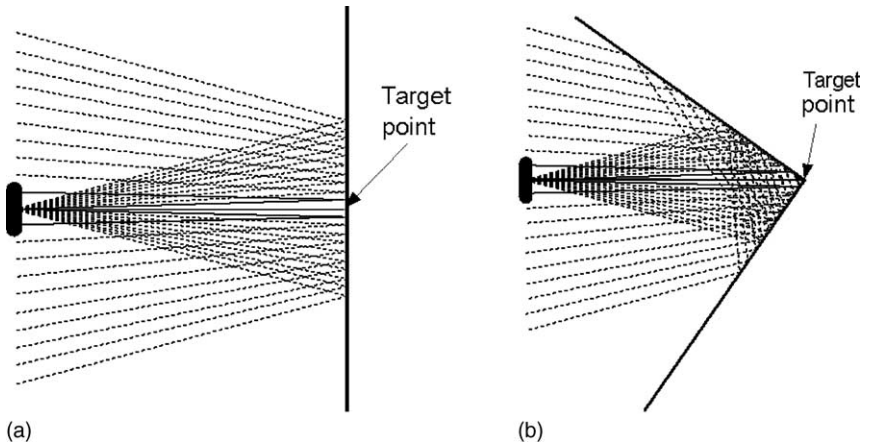

Fig. 2. Reflection of ultrasonic echoes from different surface types: (a) Wall; (b) right angle corner. Solid lines: rays that reach the transducer; broken lines: rays that do not reach the transducer.

where A is the peak amplitude of the echo obtained in the ultrasonic receiver, measured in volts. A_0 is a constant for the transducers, independent of the material or shape of the reflecting surfaces. α is the attenuation coefficient of the air (dB m^{-1}). (In this article, a value of 0.275 dB m^{-1} will be used). x is the distance between the transducers pair and the target (m). C_r is the reflection coefficient of the reflector's surface. It is a number between 0 and 1, and represents the ratio between the intensity reflected back to the transducer and the incident intensity of the acoustic beam. This single parameter includes both the absorption and the additional dispersion effects. This is an evident simplification of the complex phenomena that occur in the reflection of the ultrasonic beam. Nevertheless, this simplification will provide good results and agrees well with the experimental data obtained. N can take two values, depending on the reflector's shape: a value of 1 in the case of a wall, and a value of 2 in the case of a right corner. That is, the number of reflections of the ultrasonic beam on the target's surface before reaching the receiver. (In acute corners, N can take values higher than 2, but in this paper, these targets are not considered). θ is the angle at which the target point is viewed by the transducer.

Eq. (5) will be used in the following sections to predict the echo peak amplitude of an object placed at a distance x from the transducers, viewed at an angle θ and with a known reflection coefficient C_r.

4. Ultrasonic signal description: signal data processing and time–distance relationship

The robot YAIR[1] has a rotary ultrasonic sensor on its top [7]. The sensor has two transducers: one transmitter and one receiver, placed as shown in Fig. 3, enabling the two transducers to have the same rotating axis. This two-transducer array rotates driven by a stepper motor with 1.8° per step, giving up to 200 angular samples per scan.

At each angular position, the emitter sends a train of 16 ultrasonic pulses, with a total time of 400 μs, because the resonant frequency of the transducers is 40 kHz. The signal obtained in the receiver is amplified with programmable gain, and demodulated using the same emission frequency. Thus, the base band signal is obtained after removing the frequencies above 4 kHz from the demodulated signal. The resulting signal is then sampled at a rate of 10 k samples/s and digitized using a 12 bit A/D converter. Typically, up to 256 samples of this signal are recorded before the stepper motor advances to the next position, repeating the process. Therefore, for each angular position a vector of 256 samples is stored and processed, and the complete scan will produce an array of 200 vectors.

[1] YAIR stands for Yet Another Intelligent Robot, and is currently being developed under Spanish Government CICYT Grants DPI2002-04434-C04-03 and DROMAIN-UPV project.

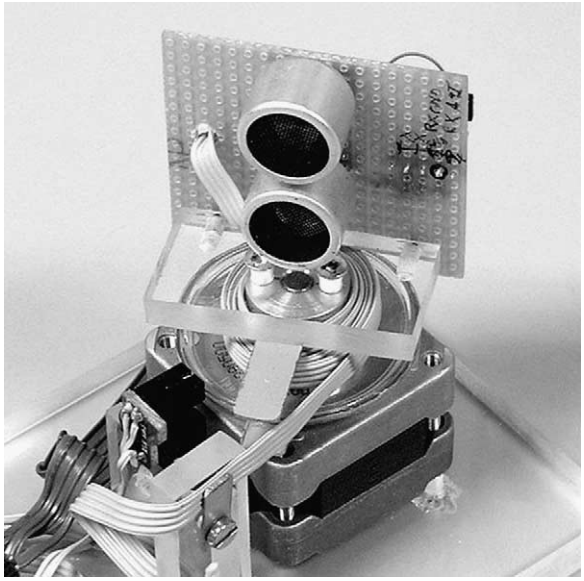

Fig. 3. Ultrasonic rotary head of YAIR robot. Note that the layout enables the two transducers to have the same rotating axis.

Given that ultrasound speed in air is c = 343 m/s at 20 °C, the distance corresponding to a sample period (t_0 = 100 μs) will be:

$$d_0 = \frac{ct_0}{2} = 0.01715\,\text{m}, \tag{6}$$

and the maximum range covered by a recorded echo will be:

$$d_{\max} = 256 d_0 = 4.39\,\text{m}. \tag{7}$$

Due to the proximity between the two transducers, while the emitter is transmitting, its vibrations are mechanically transmitted to the neighbouring receiver, obtaining high signal values that do not correspond with any target. Thus, it is necessary in practice to reject the first 25 samples (2.5 ms) of the received signal, creating a 'blind' zone $25 \times d_0$ = 0.43 m around the sensor. This is not a problem, since the sensor is placed at the geometric centre of YAIR, and its mean radius is 0.3 m. Thus, objects placed at 13 cm from the periphery of the robot will be detected and measured.

From the sampled data of an echo, the distance to the detected targets can be calculated with an accuracy of millimetres using any of the methods described in [20,22]. In our case, a simpler but accurate-enough method for map building is used:

- Taking into account that the shape and duration of any echo is always the same, the time elapsed between the beginning of an echo and its peak value will also be the same (t_{offset}) and is known *a priori* (in our case, t_{offset} = 400 μs, equivalent to four sampling periods).
- Thus, to compute the distance to a target, it is enough to find the peak amplitude of an echo, obtaining the time-of-flight using the following formula:

$$\text{ToF} = t_{\text{peak}} - t_{\text{offset}}. \tag{8}$$

- Finally, the distance to the target will be computed as follows:

$$d = \frac{c\,\text{ToF}}{2} \tag{9}$$

This method is fast, but the distance resolution is equal to d_0 (1.7 cm). Assuming random error distribution, the standard error of the readings will be: $\varepsilon_{\text{d}} \approx d_0/\sqrt{12} = 0.49$ cm. This is sufficient for building maps with grid sizes over 2 cm. If better resolution is needed, interpolation methods can be used instead.

Thus, the only digital signal processing needed is to subtract the t_{offset} value from time when each sample is taken in a complete scan, which is equivalent to make a shift of 4 samples in each vector. In this way, each peak will correspond in time with the distance from a target.

Fig. 4 shows the typical aspect of the data obtained in an ultrasonic scan from the YAIR sensor. As shown in Fig. 4a, the two walls and the corner are detected, as expected. Note that in the 3D representation of Fig. 4b, the echoes are grouped forming 'mountains' and the exact position of the target points correspond to the relative maximums of each 'mountain'.

Also, note the different amplitude of the targets: the peak corresponding to the closest wall (wall A) is the largest, wall B has a medium peak value, and the peak corresponding to the corner has the smaller peak value.

5. Application of the model: distinguishing between walls and corners

In this paper, only two types of targets are assumed as representative of the main part of the scene: walls and corners. In fact, the target points detected in scanned scenes come mainly from targets with a

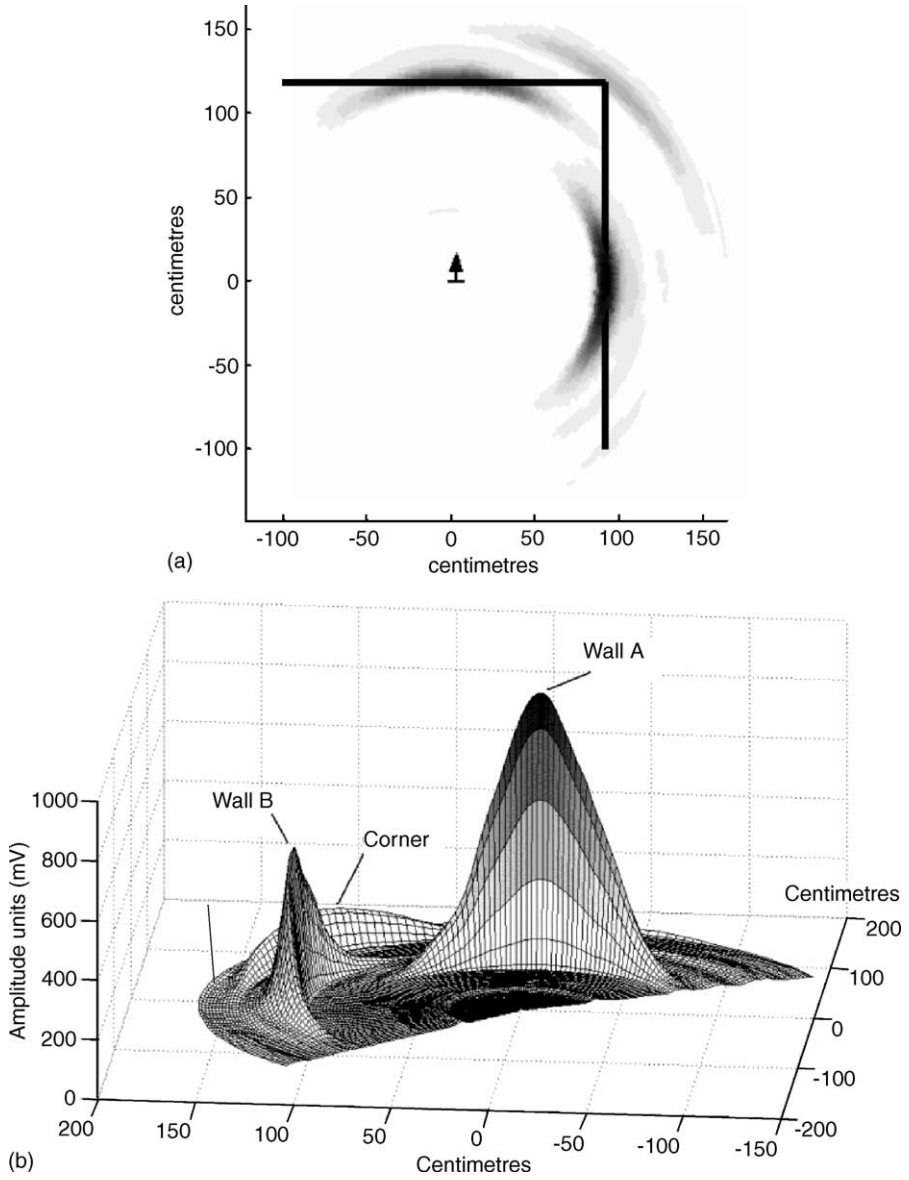

Fig. 4. Typical ultrasonic data after scanning a room's corner. (a) Horizontal layout with the walls superimposed. Note the coincidence of the signal peaks with the walls and the corner. (b) 3D view of the same map, showing the different amplitudes of the echoes and their angular evolution.

single reflection (flat surfaces) or targets with two reflections (right corners). The flat surface amount needed to produce an echo is small enough to represent almost any form of room outline as if it were formed by small flat pieces. Acute corners produce more than three reflections, and thus, the final intensity received is considerably reduced. Edges are targets that produce much lower amplitude echoes. In our approach, only echoes with amplitudes large enough to be considered as walls or as corners were taken into account, disregarding echoes with lower amplitudes, considered as noise for map building purposes.

Eq. (5) models the theoretical behaviour of the echo peak amplitudes. This equation can be used to predict

the readings obtained from a given scene or, even more important, to identify the type of target which produces a given echo. In the first case, it is necessary to know the parameters of each target: distance x, reflection coefficient C_r, exponent N (1 for walls, 2 for corners), and the angle θ at which the target point is observed by the transducer. From these parameters, and using Eq. (5), the predicted value of the echo peak amplitude can be obtained.

For the second case—the classification problem after a reading A has been taken—only one of the above mentioned parameters is needed: the reflection coefficient C_r. In effect, distance x is a datum obtained from the ToF of the echo, and angle θ is not needed anymore *if the reading A corresponds to an angle* $\theta = 0^\circ$. This is possible if a complete scan has been taken, since the peaks of the scanned 'mountains' will always correspond to a zero sight angle with the target point. Under these conditions, the value of N can be derived from Eq. (5), as the next equation shows:

$$N = \frac{(\ln(2Ax)/A_0) + 2\alpha x}{\ln C_r} \tag{10}$$

A value of 1 for N means that the target point is a wall (or a flat surface) and a value of 2 indicates a corner, or a surface with two ultrasonic beam reflections. Of course, the measured data will have added noise, some due to the measurement process, and most due to the non-uniform value of C_r in all the surfaces; and in practice, the values of N obtained from Eq. (10) will have some added noise. Grouping the experimental results of real walls and of real corners, each target category will present a statistical distribution grouped around the values 1 and 2, respectively. Fig. 5 shows the experimental distribution values of N obtained using 102 readings from corners and 206 readings from concrete walls (with a calculated $C_r = 0.59$ and a standard deviation of 0.09). The resulting shape agrees well with the theoretical result predicted by the model.

Each distribution—which is supposed in this paper to be Gaussian—will have its mean and its standard deviation. If the assumptions made about the model are valid, the mean value of N for walls must be close to 1, and for corners must be close to 2. The standard deviations obtained in the distributions of the results will be strongly dependent on the uniformity of the walls and the corners in the scene, and this fact must be taken into account for the classification of the targets.

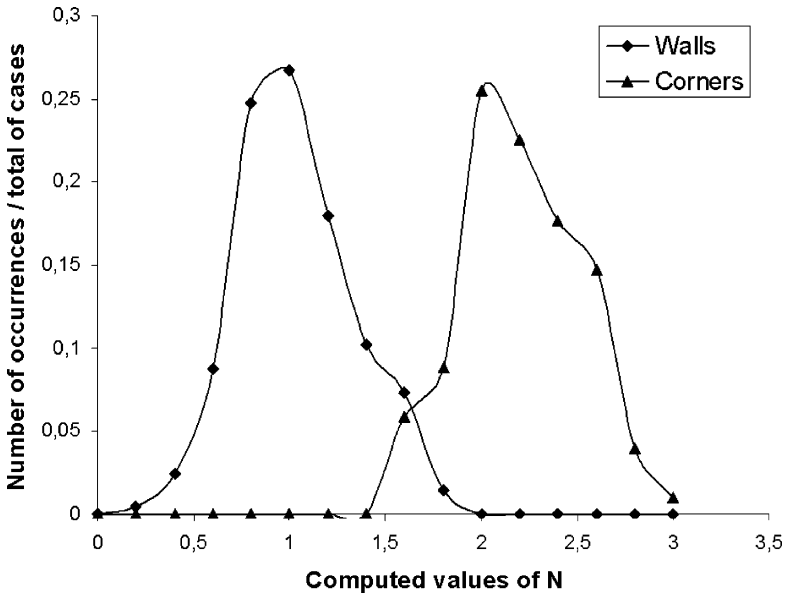

Fig. 5. Experimental results show that the computed values of N are grouped around the value of 1 for walls, and around 2 for corners, as predicted by the model. The data were obtained after 102 readings from corners and 206 readings from walls. The material was concrete, with a calculated $C_r = 0.59$.

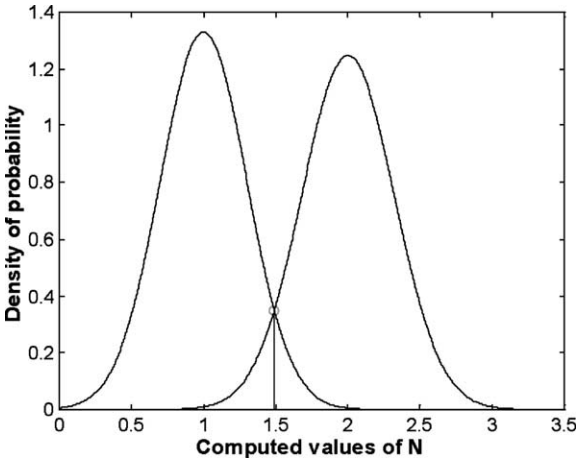

Fig. 6. Example plot of two normal distributions corresponding to values of N for walls (mean $m_1 = 1$) and corners (mean $m_2 = 2$); (arbitrary standard deviations $\sigma_1 = 0.3$ and $\sigma_2 = 0.32$ have been elected). The intersecting point ($N_0 = 1.49$ in this example) will be the limit value to classify targets as walls or as corners.

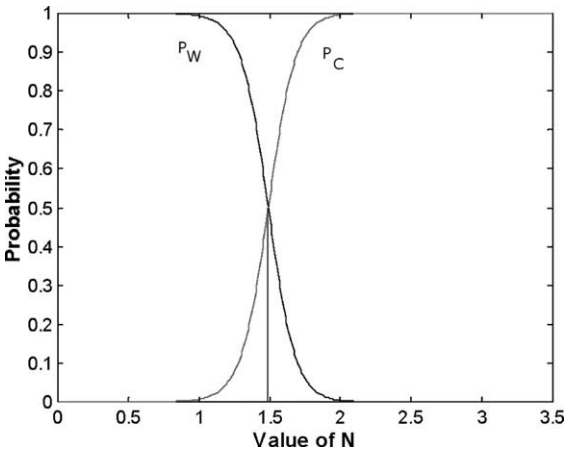

Fig. 7. Membership functions derived from the Gaussian distributions of Fig. 6.

Let us define m_1 as the mean value of the experimental distributions of N for the walls in a scene, and m_2 for the corners (i.e., m_1 will be close to 1 and m_2 will be close to 2). And σ_1 and σ_2 will be the corresponding standard deviations.

In Fig. 6, two normal distributions have been plotted as an example, taking $m_1 = 1$ and $m_2 = 2$; and $\sigma_1 = 0.3$ and $\sigma_2 = 0.32$ (arbitrary values). There is an intersection point between both distributions. Let us call N_0 to the abscissa of this point. A target with a calculated value of $N = N_0$, will have the same probability of being a wall or a corner. Thus, targets with N values above N_0 will have more probabilities of being a corner than a wall, and N values below this limit will indicate more probabilities of being a wall. In Fig. 7, the membership functions of each class corresponding to the distributions of Fig. 6 have been calculated as a function of N, showing the probabilities of being a wall (P_W) or a corner (P_C). Of course, since only two types of targets are being considered, it must always follow that: $P_W + P_C = 1$.

Also, note that for $N = N_0$, $P_W(N_0) = P_C(N_0) = 0.5$. Using these membership functions, the final information supplied to the local map and to the fusion process will be not only which type of target has been detected, but also its probability. This latter aspect can be of great utility in the sensor fusion processes.

6. Model parameters estimation procedure

The application of the model proposed requires previous knowledge of the reflection coefficient C_r, and the assumption that all the walls and corners of the environment are made of the same material, and that this is uniform in all its surfaces. If a scene fails to meet these restrictions, the expected results in the classification will be poorer. These restrictions are somewhat strong, but applying optimal estimation procedures, the parameter C_r can be dynamically estimated, improving the classification results. When different materials occur in the same scene, C_r can take the mean value of the different materials. The experiments conducted showed that the variability of C_r from one material to another is of the same order of magnitude as the C_r of the same material in most cases. Thus, the use of C_r mean values will give poorer though still acceptable results in the final map.

The procedure to obtain an estimate of C_r from a given material is simple, and can be undertaken offline. Previous knowledge of A_0 is assumed at sensor's calibration time. In our case, the value obtained was $A_0 = 3.948$ V m, after exhaustive tests in the laboratory. The value of air attenuation α was also measured, obtaining $\alpha = 0.275\,\mathrm{dB\,m^{-1}}$.

C_r can be obtained from only one ultrasonic reading from a wall oriented normal to the transducer, at a given distance x (calculated from the reading, using the ToF method). Given that N for a wall is 1 and that $\theta = 0^\circ$,

Table 1
Experimental values of C_r and their standard deviation for some common materials

Material	C_r (mean)	S.D.
Railite®	0.76	0.03
Glass	0.71	0.10
Polished plastic	0.64	0.06
Pladur®	0.62	0.07
Concrete	0.59	0.09
Cork	0.57	0.07
Natural Wood	0.51	0.04
Matt Plastic	0.47	0.06

we can use Eq. (5) to obtain C_r from the value of A obtained from the echo, as follows:

$$C_r = \frac{A}{A_0} 2x\, e^{2\alpha x} \tag{11}$$

In fact, this method is applicable in all the cases where the target point is known to be a wall, enabling the on-line estimation of C_r. However, as C_r shows significant variability in its value, it is highly recommendable to take sufficient number of readings before making an estimate for C_r. Using the above method, several materials encountered in diverse rooms, offices and corridors of our university were measured and the results obtained for C_r and their standard deviation are shown in Table 1.

7. Obtained results and discussion

Fig. 8 shows the peak amplitude values obtained from walls and corners, corresponding to a test conducted in a room whose walls are made of concrete. As it can be observed, the points are grouped around the two solid lines obtained from Eq. (5) for walls (upper line) and for corners (lower line). Some of the readings corresponding to a wall overlap with those corresponding to a corner, and vice-versa. In these cases, the classification algorithm fails, but in most cases, the types of targets can be clearly differentiated.

The model was also tested in several rooms of our department, made mainly of the same material (concrete). In these experiments, the robot was guided following different trajectories, and numerous scans were taken to distinguish and classify detected obstacles as walls or as corners. The classification results are shown in Table 2, and are very satisfactory.

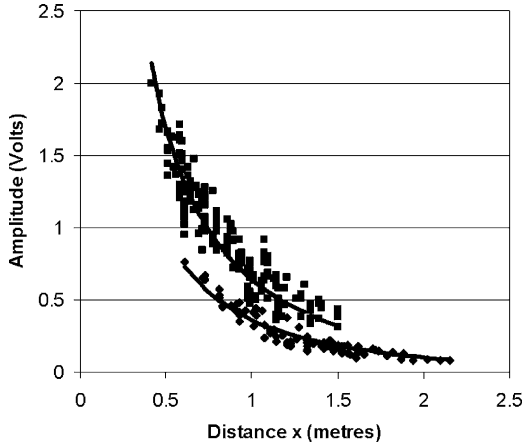

Fig. 8. Amplitude vs. distance in walls and corners. Solid lines correspond to model of walls (upper line) and to model of corners (lower line); squares: readings from walls; diamonds: readings from corners.

Table 2
Classification results obtained in a room with concrete walls (C_r = 0.59)

Obstacle type	Classified as	
	Wall (%)	Corner (%)
Wall	98	2
Corner	9	91

To test other non-homogeneous environments, another room was selected whose walls are made with fragments of Pladur® together with glass (windows) and metal stripes as well as Railite® (door panels), assuming in this case, a mean value of C_r = 0.62. The classification results are summarized in Table 3.

Finally, the results of the scans made to a group of different rooms, of different materials, using their mean value (C_r = 0.64), are summarized in Table 4, grouped by distance intervals, and the global results. The results are fairly satisfactory in most cases, providing good-enough classification results.

Table 3
Classification results obtained in a room with walls made of Pladur®, metal and railite® ($C_{r\,MEAN}$ = 0.62)

Obstacle type	Classified as	
	Wall (%)	Corner (%)
Wall	99	1
Corner	14	86

Table 4
Classification results obtained in several rooms

Obstacle type	All distances		0 m< D < 1 m		1 m < D < 1.5 m		1.5 m < D < 2 m	
	Wall (%)	Corner (%)	Wall (%)	Corner (%)	Wall (%)	Corner (%)	Wall (%)	Corner (%)
Wall	86	14	82	18	92	8	89	11
Corner	33	67	18	82	36	64	39	61

Classified as walls and corners made of different materials: pladur, concrete, metal, glass and railite. $C_{r\,MEAN}$ in this case was 0.64.

The use of a mean value for C_r when different materials are present in a given environment simplifies the recognition algorithm, but it will logically produce poorer classification results. However, as Table 1 shows, the standard deviation of the experimental C_r values is about the same order of magnitude than the differences between the C_r of different materials. This fact makes acceptable the use of a mean C_r value of the materials present in a given scene. The obtained results obtained with this simplification are good-enough, as Tables 2–4 show us.

Using the membership functions derived from the Gaussian distributions of a given room material, not only the classification as a wall or as a corner is obtained, but also their associated probability, as previously indicated. Using this procedure, a probabilistic grid map of a room was obtained, fusing all the results obtained in a robot's walk, by simply averaging the probability values obtained for each grid cell.

Fig. 9 shows the results of this test, obtained in a room made of concrete, metal and Railite®. The C_r used in this case was 0.62. As a simplification of the world, only two types of objects were considered: Walls or Corners. Thus, using only the probability of being a wall (P_W) is enough to represent the world: a value of 0 means that the object is a corner, whereas a value of 1 indicates a wall, and a value of 0.5 means the same probability of being a wall or a corner. Grid cell size is 4 cm.

This Fig. 9 represents the probability values of each cell using grey-colour scale: the values closer to 1.0 are light-coloured, whereas values closer to 0.0 are dark-coloured. When program starts, the value for each cell in the grid map is initialised to 0.5 (50% grey coloured). The results obtained seem good, although

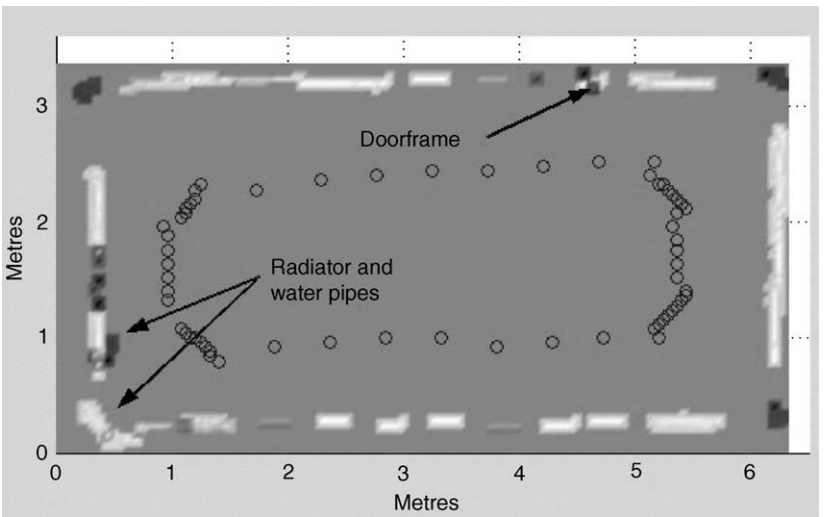

Fig. 9. Grey colour grid map showing the classification results obtained in a room made of concrete, metal and Railite®. The circles show the walk of the robot during the measurements. The cell grey level shows the probability of being a wall or a corner. White colour means high probability of being a wall, whereas black colour means high probability of being a corner. Grey colour indicates intermediate probability.

some false corners or walls, caused by the presence of disturbing objects, like radiators and vertical heat water pipes, are detected. These false detections can be corrected later, using higher-level geometric reasoning algorithms. As an example, the false wall detected in the lower-left corner of Fig. 9 can be discarded, because this point is placed in the intersection of two detected walls, and it must be a corner instead. Also, a false corner detected in the middle of a wall can be discarded by geometric considerations.

8. Conclusions

This paper analyses the amplitude of ultrasonic echoes, and describes a simple model to predict the shape and amplitude of echoes received from different materials in environments composed of walls and corners. Using this model it is possible to distinguish between walls and corners in a single circular scan of a single ultrasonic transducer pair. The parameters of the model were obtained after exhaustive tests on different materials and surfaces. Finally, the paper presents the experimental results of wall–corner classifications obtained in real tests during the walk of a mobile robot. The results suggest that the method proposed can be of great interest for map building in robotics.

The application of the model requires previous knowledge of the reflection coefficient C_r, and the assumption that all the walls and corners of the environment are made of the same material. Uniformity in all the surfaces is also required. If a scene fails to meet these restrictions, the expected results in the classification will be poorer. Parameter C_r can also be dynamically estimated, improving the classification results. For different materials in the same scene, C_r will take the mean value of the different materials.

References

[1] H. Akbarally, L. Kleeman, A sonar sensor for accurate 3D target localisation and classification, Proceedings of the IEEE International Conference on Robotics and Automation, Nagoya, Japan, 1995, pp. 3003–3008.
[2] C. Barat, N.A. Oufroukh, Classification of indoor environment using only one ultrasonic sensor, Proceedings of the IEEE Instrumentation and Measurement, Technology Conference, 2001, pp. 1750–1755.
[3] B. Barshan, B. Ayrulu, S.W. Utete, Neural network-based target differentiation using sonar for robotics applications, IEEE Trans. Robot. Autom., 2000, pp. 435–442.
[4] O. Corion, A.M. Desodt, D. Jolly, Using ultrasonic for the recognition of a real space, Proceedings of the IMEKO Sixth International Symposium Measurement and Control in Robotics, 1996, pp. 415–420.
[5] A.P. Cracknell, Ultrasonics, Wykeham Publublication Ltd., London, 1982.
[6] A. Elfes, Sonar-based real-world mapping and navigation, IEEE J. Robot. Autom. RI-3 (3) (1987) 249–265.
[7] J.A. Gil, A. Pont, G. Benet, F.J. Blanes, M. Martínez, A Can Architecture for an Intelligent Mobile Robot, Proceedings of the Third IFAC Symposium in Intelligent Components and Instruments for Control Applications (SICICA'97), 1997, pp. 65–70.
[8] F.E. Gueuning, M. Varlan, Accurate distance measurement by an autonomous ultrasonic system combining time-of-flight and phase-shift methods, IEEE Trans. Instrum. Measure. 46 (6) (1997) 1236–1240.
[9] A. Heale, L. Kleeman, Fast target classification using sonar, Proceedings of the IEEE/RSJ International Conference on Intelligent Robots and Systems, 2001, pp. 1446–1451.
[10] H. Hua, Y. Wang, D. Yan, A low-cost dynamic range-finding device based on amplitude modulated continuous ultrasonic wave, IEEE Trans. Instrum. Measur. 51 (2) (2002) 362–367.
[11] Joong Hyup Ko, Kim Wan Joo, Chung Myung Jin, A method of acoustic landmark extraction for mobile robot navigation, IEEE Trans. Robot. Autom. 12 (3) (1996) 478–485.
[12] L. Kleeman, Scanned Monocular Sonar and the Doorway Problem, Proceedings of the IEEE/RSJ International Conference on Intelligent Robots and Systems, (IROS'96), 1996, pp. 93–103.
[13] L. Kleeman, R. Kuc, Mobile robot sonar for target localization and classification, Int. J. Robot. Res. 14 (4) (1995) 295–318.
[14] R. Kuc, A spatial criterion for sonar object detection, IEEE Trans. Pattern Anal. Mach. Intell. (PAMI) 12 (7) (1990) 686–690.
[15] R. Kuc, B. Barshan, Differentiating sonar reflections from corners and planes by employing an intelligent sensor, IEEE Trans. Pattern Anal. Mach. Intell. (PAMI) 12 (6) (1990) 560–569.
[16] R. Kuc, O. Bozma, A physical model-based analysis of heterogeneous environments using sonar, IEEE Trans. Pattern Anal. Mach. Intell. (PAMI) 16 (5) (1994) 497–506.
[17] R. Kuc, O. Bozma, Building a sonar map in a specular environment using a single mobile sensor, IEEE Trans. Pattern Anal. Mach. Intell. (PAMI) 13 (2) (1991) 1260–1269.
[18] J.J. Leonard, H.F. Durrant-Whyte, I.J. Cox, Dynamic map building for an autonomous mobile robot, Int. J. Robot. Res. 11 (4) (1992) 89–96.
[19] L.C. Lynnworth, Ultrasonic Measurements for Process Control: Theory, Techniques, and Applications, Academic Press Inc., 1989.
[20] D. Marioli, E. Sardini, A. Taroni, Ultrasonic distance measurement for linear and angular position control, IEEE Trans. Instrum. Measure. 37 (4) (1988) 578–581.
[21] H.P. Moravec, A. Elfes, High resolution maps from wide angle sonar, Proceedings of the IEEE International Conference on Robotics and Automation, 1985, pp. 116–121.

[22] M. Parrilla, J.J. Anaya, C. Frish, Digital signal processing techniques for high accuracy ultrasonic range measurements, IEEE Trans. Instrum. Measure. 40 (4) (1991) 759–763.
[23] H. Peremans, K. Audenaert, J. Campenhout, A high resolution sensor based on tri-aural perception, IEEE Trans. Robot. Autom. 9 (1) (1993) 36–48.
[24] T. Yata, A. Ohya, S. Yuta, Use amplitude of echo for environment recognition by mobile robots, Proceedings of the 2000 IEEE/RSJ International Conference on Intelligent Robots and Systems, 2000, pp. 1298–1303.

Ginés Benet received the M.S. and Ph.D. degrees in Industrial Engineering from the Universidad Politécnica de Valencia, Spain, in 1980 and 1988, respectively. Since 1984, he taught computed technology and currently he is an associate professor of the Escuela Universitaria de Informática at the Universidad Politécnica de Valencia. He has been involved in several National and European research projects mainly related to Real-Time Systems and Intelligent Instrumentation. His research interests include: mobile robots, intelligent sensors, robot control and sensor data fusion.

Milagros Martínez received the M.S. degree in 1993 and Ph.D. degree in 2004, in Computer Engineering from the Universidad Politécnica de Valencia, Spain. Since 1994, she taught computers structure and she is currently an assistant professor in the Facultad de Informática at the Universidad Politécnica de Valencia. Her research interests include: mobile robots and the use of ultrasonic sensors.

Francisco Blanes received the M.S. degree in 1994 and Ph.D. degree in 2000, in Computer Engineering from the Universidad Politécnica de Valencia, Spain. Since 1995, he taught real time computer systems and he is currently an assistant professor in the Escuela Superior de Ingeniería Industrial at the Universidad Politécnica de Valencia. His research interests include: real-time robot control, perception and sensor fusion in mobile robots.

Pascual Pérez received the M.S. degree in 1998 from the Universidad Politécnica de Valencia, Spain. Since 1998, he taught computer technology at Facultad de Informática. He is currently an assistant professor in the Departamento de Informática de Sistemas y Computadores at the Universidad Politécnica de Valencia. His research interests include: real-time robot control, embedded systems and field-bus networks.

José E. Simó received the MS degree in Industrial Engineering in 1990 from the Universidad Politécnica de Valencia, Spain and Ph.D. degree in Computer Science from the same university in 1997. Since 1990, he has been involved in several National and European research projects mainly related to Real-Time Systems and Artificial Intelligence. He is currently an associate professor of Computer Engineering at the Technical University of Valencia and his current research is focused on the development of autonomous systems and mobile robots.